Available online at www.sciencedirect.com

ScienceDirect

Procedia Engineering 138 (2016) 281 – 290

Procedia Engineering

www.elsevier.com/locate/procedia

"SYMPHOS 2015", 3rd International Symposium on Innovation and Technology in the Phosphate Industry

Electrode Based on Oxyphosphates as Anode Materials for High Energy Density Lithium-ion Batteries

Karima Lasri[a], Ismael Saadoune[a]* and Kristina Edström[b]

[a]*LCME, FST Marrakech, Uni. Cadi Ayyad. Av. A: Khattabi, BP 549, 40000 Marrakech, Morocco*
[b]*Department of Chemistry - Ångström Laboratory, Uppsala University, Box 538, SE-751 21 Uppsala, Sweden*

Abstract

Lithium-ion batteries (Li-ion) are interesting devices for electrochemical energy storage for most emerging green technologies such as wind and solar technologies or hybrid and plug-in electric vehicles or for classical electrical devices such as laptops, phones or other electronic tools. Nevertheless, the oxygen release at high potentials in the present commercialized electrode materials (e.g. $LiCoO_2$) leads to high thermal instability of these oxides and thus to many safety problems. This safety problem is more pronounced for stationary applications for which large size batteries were needed. Polyanionic materials in general, and particularly phosphates were well renowned by their high structural stability which are essential to overcome the above mentioned safety issue. Here, we present the structural and the electrochemical performances of three oxyphosphates $M_{0.5}TiOPO_4$ (M: Ni, Co, Fe). More than 300 mAh/g discharge capacity could be delivered by these phosphates under relatively high cycling rate. The lithium insertion/extraction mechanism is composed from an intercalation process for low lithium content to a conversion mechanism for higher lithium concentration leading to the extrusion of the transition metal M from the structure.

Peer-review under responsibility of the Scientific Committee of SYMPHOS 2015

Keywords: Phosphates, Lithium-ion batteries, Energy storage

* Corresponding author. Tel.: +212 5 24 43 46 88 ; fax: +212 5 24 43 31 70.
E-mail address: i.saadoune@uca.ma

Peer-review under responsibility of the Scientific Committee of SYMPHOS 2015
doi:10.1016/j.proeng.2016.02.086

1. Introduction

The projected doubling of world energy consumption within the next 50 years, coupled with the growing demand for low- or even zero-emission sources of energy, has brought increasing awareness of the need for efficient, clean, and renewable energy sources. Energy based on electricity that can be generated from renewable sources, such as solar or wind, offers enormous potential for meeting future energy demands. However, the use of electricity generated from these intermittent, renewable sources requires efficient electrical energy storage
Rechargeable batteries, and especially lithium and sodium ion batteries, are interesting devices for electrochemical energy storage for most emerging green technologies such as wind and solar technologies or hybrid and plug-in electric vehicles. Compared with conventional aqueous rechargeable cells, such as nickel–cadmium and nickel–metal hydrid, Li-ion cells have higher energy densities, higher operating voltages, lower self-discharge and lower maintenance requirements [1].

From a simple description, when you charge a lithium-ion battery, the applied electrical current causes the $LiCoO_2$ cathode to lose electrons and to form lithium ions. These ions are then pushed through the electrolyte solution to the graphite anode, where they're stored. When a device – such as a computer or a cellphone – draws on the battery, the graphite releases electrons, creating an electrical current, and the lithium ions travel back to the cathode. Although the present commercial lithium-ion batteries use $LiCoO_2$ or $LiMn_2O_4$ as cathode materials, and graphite or carbonaceous materials as anode materials [2], there are a number of studied compounds that demonstrated a potential application as anode or cathode materials for such rechargeable batteries. Most of them were reported on Fig. 1.

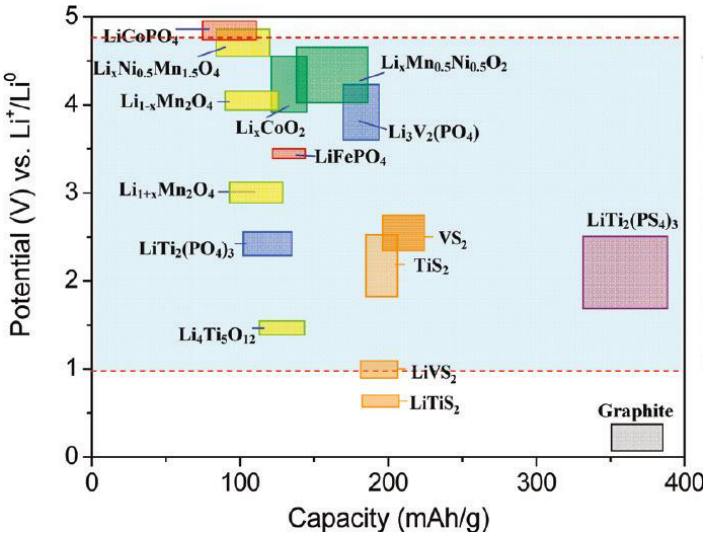

Fig. 1: Voltage versus capacity of several electrode materials [3]

Despite the early works back in 1980s [4-5], intensive studies on polyanion materials have not been conducted until recent fifteen years. These materials are receiving growing attentions because of the inherent stability of the polyanion group, which can delay or minimize the oxygen loss happening in traditional layer and spinel oxides. Indeed, with the extensive applications of lithium ion batteries, many batteries fire and explosion accidents were reported. Fig. 2 illustrates an example of the consequence of the safety issue. The safety problem of lithium ion batteries have become one main handicap in theirs dissemination. It has been demonstrated that the thermal decomposition of electrolyte, anode and cathode [6-8] is the main responsible for this safety issue.

So, further studies to ensure the safe use of lithium ion batteries were needed. From the cathode side (and sometimes from the anode side), this dangerous drawback was caused by the oxygen release from the used electrode material, especially when is based on layered oxide.

Fig. 2: Chinese Electric Bus Fire (Photo via Eastday)

Lithium transition metal phosphates are promising candidates both as positive and negative electrode materials for Li-ion batteries. The presence of $M_n(PO_4)_y$ grouping provides an excellent stability and long term cycling to this polyanionic materials in comparison to lithium transition-metal oxides, namely $LiCoO_2$ or $LiMn_2O_4$. In fact, the oxygen-phosphorous bond is more covalent in nature than polar oxygen-metal bonds. Thus, no loss of oxygen occurs from the framework, which is the responsible of the reactivity of the used electrolyte [9]. The main problem of such phosphates lies in their poor rate capability, which is attributed to their low electronic conductivity and slow kinetics of lithium-ion diffusion. Although $LiFePO_4$ was much more explored [10-11], several other lithium transition metal phosphates, including $LiFe_{0.4}Mn_{0.6}PO_4$ [12], $Li_3Fe_2(PO_4)_3$ [13], $Li_2VOP_2O_7$ [14], $Ni_{0.5}TiOPO_4$ [15] and $Fe_{0.5}TiOPO_4$ [16], have been intensively studied over the world.

In the quest for other new framework materials, candidates for the anode of the lithium batteries, based on the phosphate polyanion building block, we have investigated the electrochemical properties of $M_{0.5}TiOPO_4$ (M: Co, Ni, Fe) oxyphosphates. These functional materials were prepared directly by using the phosphoric acid as phosphorus precursor. The crystal structure of these materials and their electrochemical performance, after carbon coating, were presented.

2. Experimental

2.1. Synthesis

$M_{0.5}TiOPO_4$ (M: Co, Ni, Fe) powders were prepared by the sol-gel synthesis process. Depending on the nature of the transition metal M, commercial transition metal precursor (iron(II) acetate or nickel or cobalt nitrates) was progressively dissolved in a solution (1M) of H_3PO_4 (98%, Fluka) and $TiCl_4$ diluted in ethanol (98%, Prolabo) under constant magnetic stirring. In order to maintain pH = 0 at which the gel is formed, 1.4 ml of water was added. The gel was dried at 80°C for 8 h to remove excess ethanol. The obtained powder was ground in a mortar and put into an alumina crucible and calcined at 850°C for 18 h with intermediate mechanical grinding. The synthesis of the $Fe_{0.5}TiOPO_4$ powder was performed in an argon atmosphere while the Co- and Ni- homologous were prepared under air. After the synthesis, carbon-coated $M_{0.5}TiOPO_4$/C composites were obtained by mixing intimately $M_{0.5}TiOPO_4$ (85% wt.) and sucrose (15% wt.) in an acetone solution. The mixture was then heat-treated at 600°C for 5 h under argon. From SEM analysis of the prepared $M_{0.5}TiOPO_4$/C powders (not showed here), consists of primary particles (100-200 nm) and agglomerated secondary particles (1-2 µm) indicating the sub-micrometric structure of the powders.

2.2. Characterization

Powder X-ray diffraction patterns (XRD) were collected with a Siemens D5000 diffractometer in reflection mode using CuKα radiation. XRD patterns were collected between 10° and 100° with 0.02° step size and 30s counting time, and were refined by the Rietveld method.

Thermogravimetric (TG) analysis was performed with a Q500 Thermogravimetric Analyzer. The scans were performed at a heating rate of 15 °C/min in the temperature range from 25 to 800 °C.

The Raman spectra were collected at room temperature using a Renishaw 2000 spectrometer equipped with a 514 nm diode laser. Spectra were recorded in the 2000-200 cm^{-1} range.

2.3. Electrochemical measurements

In order to prepare the working electrode, 75% wt. of active $M_{0.5}TiOPO_4/C$ powder were dispersed in N-methyl pyrrolidone (NMP) with 15 wt.% of carbon Super P, and 10 wt.% of poly-vinylidene fluoride PVDF. This mixture was ball-milled during 45 min. The formed slurry was tape-casted onto a Cu foil and dried at 80°C. Electrode discs were cut out from the copper foil, and dried again in vacuum at 80°C for 6 hrs.

Electrochemical measurements were carried out using coin cells (CR2032). The cells were assembled in an argon filled glove box, using the as-prepared electrode as the working electrode, lithium foil as the counter and reference electrode, a porous polypropylene (Celgard 2300) as the separator, and 1M $LiPF_6$ in a 1:1 ethylene carbonate: dimethyl carbonate (EC:DEC) solution as electrolyte. The batteries were tested on a BioLogic MPG2 potentiostat in galvanostatic mode at room temperature.

3. Results and discussions

XRD patterns of the $M_{0.5}TiOPO_4/C$ powders are shown in Fig. 3. The diffraction peaks can be indexed in the monoclinic system with the space group $P2_1/c$. Few low-intensity peaks are detected in the case of $Ni_{0.5}TiOPO_4/C$ and $Co_{0.5}TiOPO_4/C$, which are mainly attributed to TiO_2 rutile, and $Ti_2P_2O_7$ respectively. The refinement of these structures with the Fullprof software shows that these impurities represent each less than 4% (in weight) in the corresponding composite. Note that no extra peaks of carbon can be observed in the XRD patterns of the studied samples, indicating that the carbon in the composite is amorphous.

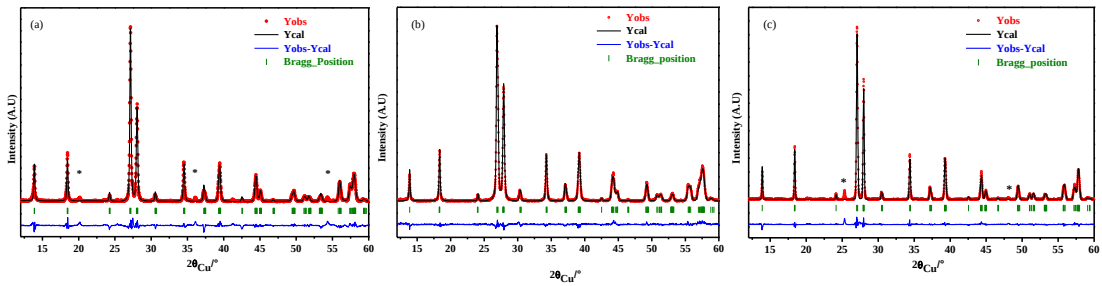

Fig. 3: XRD patterns of the synthesized $M_{0.5}TiOPO_4/C$ composites (a) $Ni_{0.5}TiOPO_4/C$; (b) $Fe_{0.5}TiOPO_4/C$; (c) $Co_{0.5}TiOPO_4/C$

The atomic positions of the three phosphates were refined. The atomic distribution within the structure is similar [17] but the unit cell parameters were quite different as the results of the difference in size between the transition metal cations. Table 1 gives the refined monoclinic unit cell parameters of the $M_{0.5}TiOPO_4$ (M: Ni, Fe, Co) electrode materials.

Table 1. Monoclinic unit cell parameters of the $M_{0.5}TiOPO_4$ (M: Ni, Fe, Co) phosphates

Type of phosphate	a (Å)	b (Å)	c (Å)	β (°)	Volume (Å^3)
$Fe_{0.5}TiOPO_4$	7.3889(8)	7.3874(8)	7.4128(8)	120.41(6)	348.72(1)
$Co_{0.5}TiOPO_4$	7.3738(7)	7.3616(6)	7.3633(6)	120,31(6)	345.91(2)
$Ni_{0.5}TiOPO_4$	7.3829(3)	7.3301(3)	7.3499(3)	120.23(2)	343.77(2)

The structure of these three phosphates is shown in Fig. 4. The 3-dimensional framework is built up from $[TiO_6]$ octahedra and $[PO_4]$ tetrahedra. $[TiO_6]$ octahedra are linked together by corners and form infinite chains along the c-

axis. These chains are linked together by [PO_4] tetrahedra. M (Fe, Co, Ni) atoms are located in octahedral sites (2a site) sharing two faces with two [TiO_6] octahedra. The material also contains octahedral vacant sites that constitute favorable way for lithium insertion. However, as many of phosphates, $M_{0.5}TiOPO_4$ exhibits a low electronic conductivity reducing notably its electrochemical performances. This low conductivity, due to the long M-M distance, was circumvented by using the carbon coating approach. It should be noticed that the average P-O distance within the PO_4 tetrahedra approaches 1.524 Å, which reflects the strong covalency of this bonding leading to the high structural stability of these phosphates. So, no oxygen release from the structure could be expected during the electrochemical cycling of theses electrode materials. This has to be considered as an advantage for the safety consideration in comparison with the layered oxides.

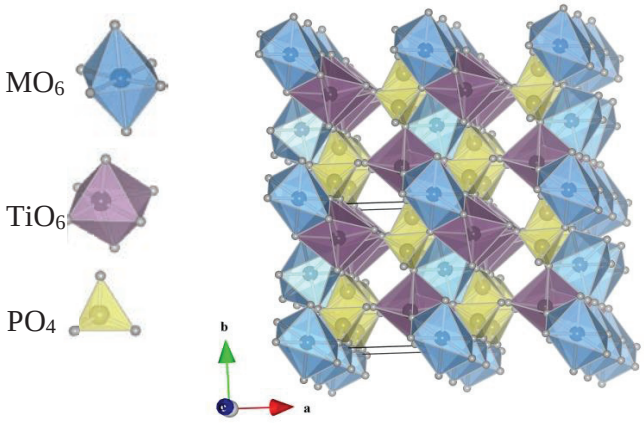

Fig. 4: Projection along the (001) plane of the crystal structure of $M_{0.5}TiOPO_4$

To estimate the amount of carbon present in the $M_{0.5}TiOPO_4$/C composite and to determine the changes in sample weight with increased temperature, TG analysis was carried out from 50 to 600 °C in air. Fig. 5 shows the TGA curves of $Ni_{0.5}TiOPO_4$ and $Ni_{0.5}TiOPO_4$/C, as example from the $M_{0.5}TiOPO_4$ (M: Fe, Co, Ni) series.

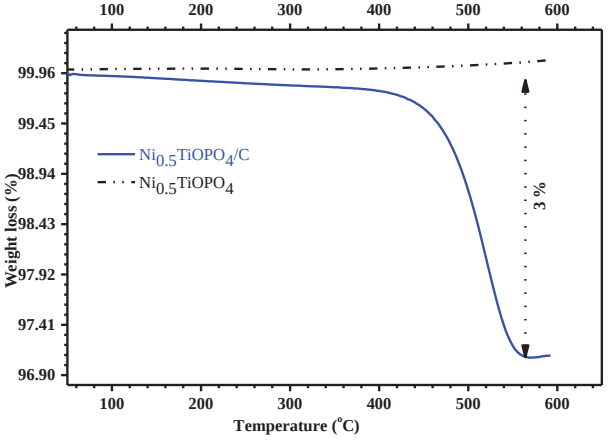

Fig. 5: TG thermograms of $Ni_{0.5}TiOPO_4$ and $Ni_{0.5}TiOPO_4$/C carried out in air.

The composite powders start to lose weight slowly at a temperature of approximately 150 °C, while the $Ni_{0.5}TiOPO_4$ powders remain stable over the whole temperature range. This weight loss is due to the oxidation of coated carbon into carbon dioxide. Therefore, the amount of amorphous carbon in the $Ni_{0.5}TiOPO_4$/C composite can be estimated to be approximately 3 wt. %. Almost the same carbon rate was obtained for $Co_{0.5}TiOPO_4$/C and $Fe_{0.5}TiOPO_4$/C.

Raman analysis was used essentially to confirm the presence of the carbon coating layer in the $M_{0.5}TiOPO_4$/C composite as the XRD study presented above gave no indication of the presence of carbon in the studied samples. Fig. 6 shows the Raman spectra of the three studied $M_{0.5}TiOPO_4$/C (M: Co, Ni, Fe) composites that clearly evidenced similar bands characteristic of the oxyphosphate. Indeed, the sharp band around 750 cm^{-1} is attributed to the vibration of the –Ti–O–Ti–O–chains, while the bending and stretching vibrations of the PO_4^{3-} group are found in 300-500 cm^{-1} and 860-1130 cm^{-1} regions, respectively. The signals located in the low wavenumber region correspond to translational vibrations of the Ti^{4+}, M^{2+} and PO_4^{3-} ions and PO_4^{3-} librations [18].

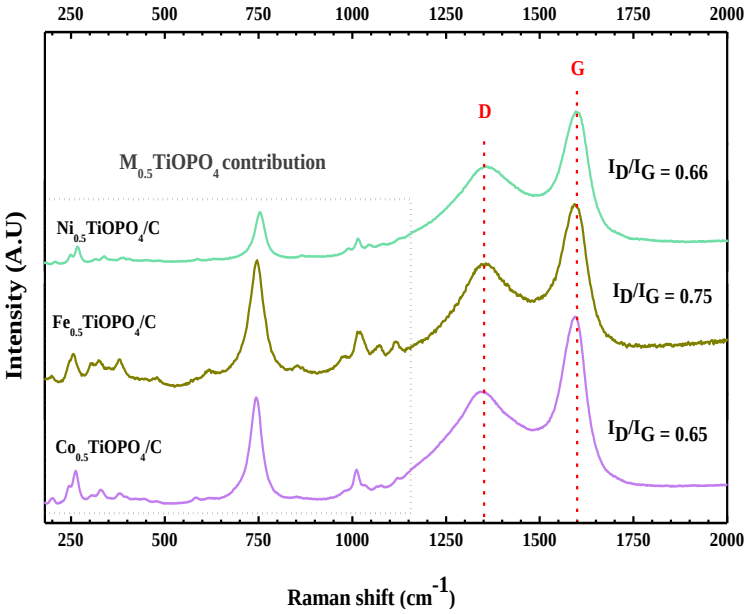

Fig. 6: Raman spectra of $M_{0.5}TiOPO_4$/C carbon composite (M = Ni, Fe and Co)

The two peaks at 1300 cm^{-1} and 1600 cm^{-1} are the D- and G-band are characteristic of carbon. The coexistence of D-band and G-band, with I_D/I_G less than 0.75, indicates the partial graphitization of carbon after treating at 600 °C. This result is a clear indication of the presence of carbon in the studied sample that was estimated from TG analysis around 3%.

The electrochemical performances of the studied composites were displayed simultaneously in Fig. 7. In general, a similar electrochemical behavior was observed for the three isostructural materials $Ni_{0.5}TiOPO_4$, $Fe_{0.5}TiOPO_4$ and $Co_{0.5}TiOPO_4$.

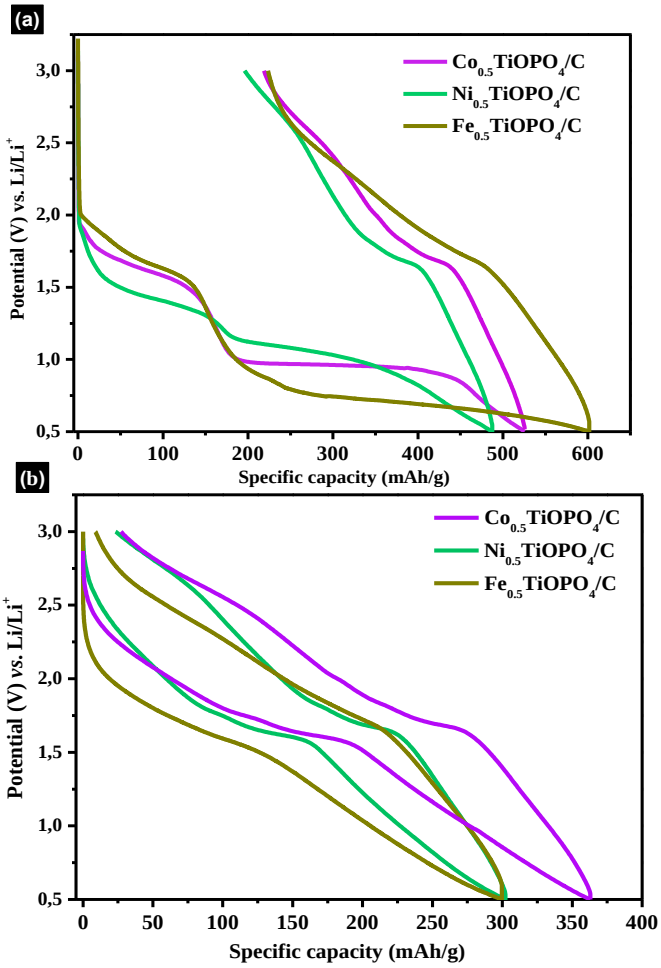

Fig. 7: Voltage versus capacity profiles of $Ni_{0.5}TiOPO_4$, $Fe_{0.5}TiOPO$ and $Co_{0.5}TiOPO$ for the 1st cycle a) and the 2nd cycle b) in the voltage window 0.5–3.0 V versus Li at C/20 current rate.

The galvanostatic measurements were carried out in half-cell in the potential window from 0 5 to 3V. As can be seen, the evolution of the potential versus lithium composition highlights two pseudo-plateau during the discharge process, corresponding to the insertion of one Li^+ and around three Li^+ ions per formula unit (f.u.).

During the charge, 2.5 Li^+/f.u. are extracted from the electrode with a single pseudo-potential plateau around 1.8 V vs. Li^+/Li. Note that the loss of capacity during the first electrochemical cycle is about 30% for the three materials. The second discharge profile is distinctly different from that of the first with a single pseudo-potential around 1.8 V vs. Li^+/Li. The profile of the voltage vs. capacity remains unchanged in the subsequent cycles, indicating the reversibility of electrochemical process.

The origin of this irreversibility was elucidated via the study of the lithiation/delithiation reaction mechanism in these phosphates where the extrusion of M metal (M: Fe, Co, Ni) was clearly evidenced [16,19,20]. In the case of $Ni_{0.5}TiOPO_4$ for example, a recent detailed in-situ spectroscopic studies revealed that the large initial irreversible capacity loss is attributed to formation of the Ni clusters and to SEI (Solid Electrolyte Interphase). XANES results show that, in addition to the reduction of Ti^{4+} to Ti^{3+} and to Ti^{2+} during the lithiation process, the PO_4 units were also

involved in the redox reactions being partially participating in the irreversible reactions. Correlating the HAXPES results to the plateaus in the galvanostatic discharge/charge voltage profile indicates a combined cooperative contribution from Ni and Ti in both plateaus; however, the first plateau is dominated by the reduction of Ti while the second is dominated by reduction of Ni^{2+} to Ni^0. These results were confirmed by the Mössbauer study done in the case of the Fe-based oxyphosphate $Fe_{0.5}TiOPO_4$. In fact, a series of $Li_xFe_{0.5}TiOPO_4$ (x = 0.06, 0.22, 0.76, 1.14) were chemically prepared and analyzed by X-ray diffraction [16]. A structure amorphisation of the $Li_xFe_{0.5}TiOPO_4$ phosphates takes place during the lithiation process. Magnetization and Mössbauer spectroscopy studies of the $Li_xFe_{0.5}TiOPO_4$ samples evidenced the formation of iron metal which induces a deterioration of the crystal structure of the studied electrode materials. The lithiation process leads to a conversion reaction, which is the origin of the irreversibility of the electrochemical process during the first discharge. An in-situ structural analysis during the cycling of the $Li//Fe_{0.5}TiOPO_4$ electrochemical cell, cycled in different potential windows, was recently performed showing the progressive amorphization of the phosphate structure upon lithium insertion [21].

In terms of cycling performance in the potential range [0.5-3V], $Li//Ni_{0.5}TiOPO_4/C$, $Li//Fe_{0.5}TiOPO_4/C$ and $Li//Co_{0.5}TiOPO_4/C$ respectively deliver a specific capacity of 249, 297 and 263 mAh/g obtained after 17 cycles under the moderate electrochemical rate of C/10 as elucidated in Fig. 8.

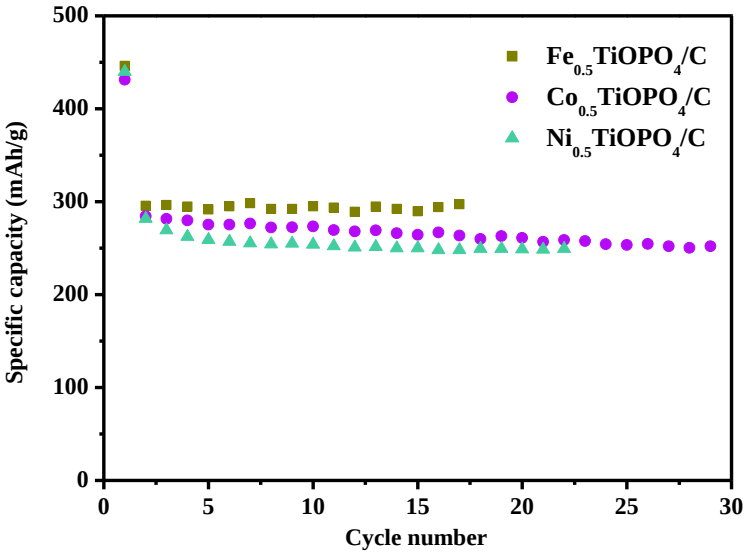

Fig. 8: Discharge capacity versus cycle number plots of $Ni_{0.5}TiOPO_4/C$, $Fe_{0.5}TiOPO_4/C$ and $Co_{0.5}TiOPO_4/C$ at C/10 current rate in the voltage range of 0.5–3.0 V.

These values are low compared to those obtained in the case of graphite for which the experimental capacities is close to 370 $mAh.g^{-1}$ but the studied electrode materials have better capability to cycle even at faster cycling regimes (5C). Figure 10 shows the evolution of the specific capacity during galvanostatic cycling for a selected three materials for the mentioned regime. An electrochemical rate capability test was carried out on the environmentally benign $Fe_{0.5}TiOPO_4$. The evolution of the specific capacity with cycling at different rates was plotted in Fig. 9.

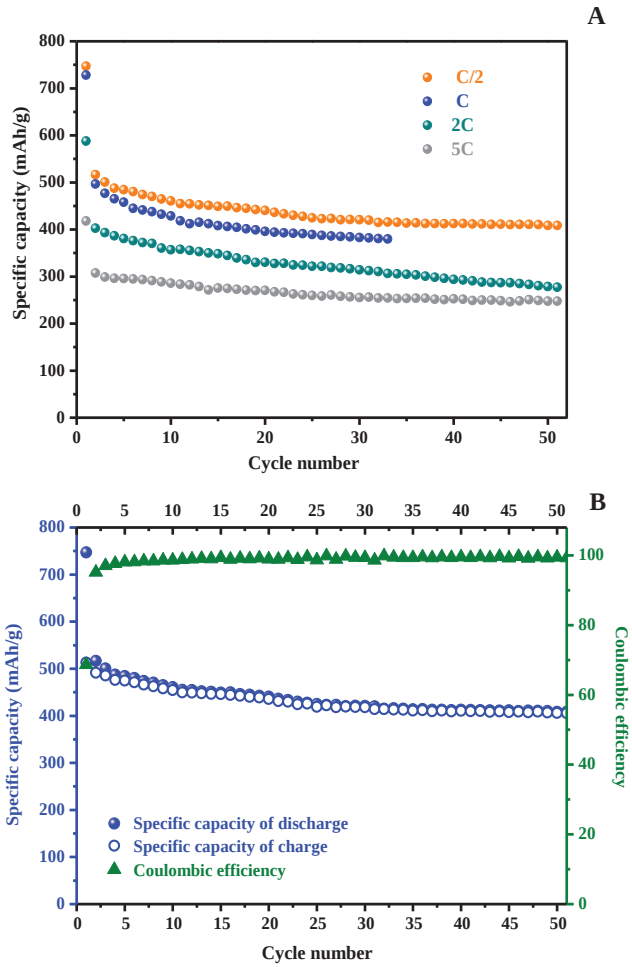

Fig. 9: Discharge capacity versus cycle number of Li//$Fe_{0.5}TiOPO_4$/C cell in the potential window [3.0-0.02V] (A) at different rate (B) Coulombic efficiency with cycle number at C/2 rate.

$Fe_{0.5}TiOPO_4$/C exhibits significantly excellent electrochemical performance with a specific capacity around 450 mAh/g at C/2. The discharge capacity loss is less than 15% after 50 cycles starting from the second cycle.

The discharge capacity at the second cycle decreases from 505, 490, 420 and 305 mAh/g for C/2, 1C, 2C and 5C rates to 430, 395, 300 and 260 mAh/g at the 30^{th} cycle. The capacity retention is also excellent under C/2 rate with a coulombic efficiency approaching 95%. These good energetic performances, which are slightly different for the other studied phosphates, clearly show that these electrodes are candidates for the anode electrode for high energy density batteries.

4. Conclusion

$M_{0.5}TiOPO_4$ (M: Fe, Co, Ni) anode materials were successfully prepared by a sol-gel method directly from the phosphoric acid by controlling the pH and synthesis temperature. Structural study by the Rietveld method shows that these phosphates crystallize in the monoclinic system (S.G. $P2_1/c$) with unit cell parameters depending on the nature of the transition metal M. A highly covalent P-O bonding in these structures explains the reason of their structural

and thus thermal stability of these electrode materials. In order to overcome the low electronic conductivity of the studied samples, a carbon-coating method was used to prepare the $M_{0.5}TiOPO_4$/C composite. The presence of carbon was clearly evidenced by Raman spectroscopy and its amount in the composite was deduced from the TG analysis of the samples in air. The $M_{0.5}TiOPO_4$/C composites display excellent Li storage properties with considerable capacity of more 250 $mAh.g^{-1}$ after 50 discharge/charge cycles at 5C rate. By decreasing the particle size ($\leq$ 200 nm), which facilitate the insertion/disinsertion processes of Li^+ ions, these composites reveal enhanced electrochemical performances and high cycling stability compared to those prepared using the solid-state methods [16] with large particle size. In-situ structural studies reveal that the irreversibility during the first cycle is attributed to the extrusion of the transition metal (Ni, or Fe or Co) from the structure leading to an amorphisation of the structure that behaves as an excellent host matrix for the subsequent cycles.

Acknowledgements

The authors would like to thank IRESEN Institute and CNRST-Morocco for their financial support

References

[1] J. M. Tarascon and M. Armand, Issues and challenges facing rechargeable lithium batteries Nature, 404 (2001) 359-367.
[2] T. Nagaura, K. Tozawa, Lithium ion rechargeable battery, Prog. Batt. Solar Cells, 9 (1990) 209-213.
[3] J. B. Goodenough, Y. Kim, Challenges for Rechargeable Li Batteries, Chem Mater, 22 (2010) 587–603
[4] A. Manthiram, J.B. Goodenough, Lithium insertion into $Fe_2(SO_4)_3$-type frameworks, J. Power Sources 26 (1989) 403–408.
[5] C. Delmas, A. Nadiri, J.L. Soubeyroux, The NASICON-type titanium phosphates $ATi_2(PO_4)_3$ (A=Li, Na) as electrode material, Solid State Ionics 28 (1988) 419–423.
[6] Kawamura, T., Kimura, A., Egashira, M., Okada, S., and Yamaki, J.I., Thermal Stability of Alkyl Carbonate Mixed-solvent Electrolytes for Lithium Ion Cells, J. Power Sources, 104(2002) 260-264
[7] Jiang, J.W., and Dahn, J.R., Effects of Solvents and Salts on the Thermal Stability of LiC_6, Electrochim. Acta, 49 (2004) 4599-4604.
[8] Baba, Y., Okada, S., Yamaki, J., Thermal Stability of Li_xCoO_2 Cathode for Lithium Ion Battery, Solid State Ionics, 148 (2002) 311-316.
[9] H. Huang, T. Faulkner, J. Barker and M.Y. Saidi, Lithium metal phosphates, power and automotive applications, J. Power Sources 189 (2009) 748-751.
[10] A.S. Andersson, J.O. Thomas, The source of first-cycle capacity loss in $LiFePO_4$, J. Power Sources 97–98 (2001) 498-502.
[11] K. Zaghib, K. Striebel, A. Guefi, J. Shim, M. Armand, M. Gauthier, $LiFePO_4$/polymer/natural graphite: low cost Li-ion batteries, Electrochim. Acta 50 (2004) 263-270
[12] I. Bezza, M. Kaus, R. Heinzmann, M. Yavuz, M. Knapp, S. Mangold, S. Doyle, C.P. Grey, H. Ehrenberg, S. Indris, I. Saadoune, Mechanism of the delithiation/lithiation process in $LiFe_{0.4}Mn_{0.6}PO_4$: In situ and ex situ investigations on long-range and local structures, J. Phys. Chem. C, (2015) DOI: 10.1021/jp513032r
[13] K. S. Nanjundaswamy, A. K. Padhi, J. B. Goodenough, S. Okada, H. Ohtsuka, H. Arai, J. Yamaki , Synthesis, redox potential evaluation and electrochemical characteristics of NASICON-related-3D framework compounds, Solid State Ionics 92 (1996) 1-10.
[14] M. Satya Kishore, V. Pralong, V. Caignaert, U.V. Varadaraju, B. Raveau, A new lithium vanadyl diphosphate $Li_2VOP_2O_7$: synthesis and electrochemical study, Solid State Sciences 10 (2008) 1285-1291
[15] K. Lasri, M. Dahbi, A. Liivat, D. Brandell, K. Edström, I. Saadoune, Intercalation and conversion reactions in $Ni_{0.5}TiOPO_4$ Li-ion battery anode materials, J. Power Sources 229, (2013) 265-271.
[16] K. Lasri, I. Saadoune, Y. Bentaleb, D. Mikhailova, H. Ehrenberg, L. Häggström and K. Edström, Origin of the irreversible capacity of the $Fe_{0.5}TiOPO_4$ anode material, Solid State Ionics, 224, (2012)15-20.
[17] K. Maher, K. Edström, I. Saadoune, T. Gustafsson, and M. Mansori, The electrochemical behaviour of the carbon-coated $Ni_{0.5}TiOPO_4$ electrode material, J. Power Sources, 196 (2011) 2819-2825.
[18] A. El Jazouli, S. Krimi, B. Manoun, J.P. Chaminade, P. Gravereau, D. de Waal, Preparation and structural characterization of two new titanium phosphates $NaCa_{0.5}Ti(PO_4)_3$ and $Ni_{0.5}TiOPO_4$, Ann. Chim. Sci. Mat. 23 (1998) 7-10.
[19] R. Eriksson K. Lasri, M. Gorgoi, T.Gustafsson,, K. Edström, D. Brandell, I. Saadoune and M. Hahlin, Electronic and Structural Changes in $Ni_{0.5}TiOPO_4$Li-Ion Battery Cells Upon First Lithiation and Delithiation, Studied by High-Energy X‐ ray Spectroscopies, J. Phys. Chem. C, , , DOI DOI: 10.1021/jp511170m (2015).
[20] R. Essehli, B. El Bali, H. Ehrenberg, I. Svoboda, N. Bramnik, H. Fuess, $Co_{0.5}TiOPO_4$: Crystal structure, magnetic and electrochemical properties, Mat. Res. Bull, 44 (2009) 817-821.
[21] K. Lasri, A. Mahmoud, I. Saadoune, M.T. Sougrati, L. Stievano, P.-E. Lippens, R. P. Hermann, H. Ehrenberg, Toward understanding the lithiation/delithiation Process in $Fe_{0.5}TiOPO_4$/C electrode material for lithium-ion batteries, Solar Energy Materials and Solar Cells, accepted (2015)